Infrared Spectra of Transition-Metal Dioxide Anions: MO_2^- (M = Rh, Ir, Pt, Au) in Solid Argon

Yu Gong and Mingfei Zhou*

Department of Chemistry, Shanghai Key Laboratory of Molecular Catalysts and Innovative Materials, Advanced Materials Laboratory, Fudan University, Shanghai 200433, People's Republic of China

Received: February 2, 2009; Revised Manuscript Received: February 27, 2009

Transition-metal dioxide anions RhO_2^-, IrO_2^-, PtO_2^-, and AuO_2^- were produced from cocondensation of laser-ablated metal atoms and electrons with dioxygen in excess argon at 6 K. Photosensitive absorptions were assigned to the antisymmetric stretching vibration (ν_3) of the metal dioxide anions from isotopic shifts and splittings as well as theoretical frequency calculations. On the basis of the observed ν_3 vibrational frequencies for $M^{16}O_2$ and $M^{18}O_2$, the anions are estimated to be linear or near linear. Density functional calculations at the DFT/B3LYP level predicted that the third-row transition-metal dioxide anions IrO_2^-, PtO_2^-, and AuO_2^- have singlet, doublet, and triplet ground states with linear structures, while the RhO_2^- anion was predicted to have a slightly bent geometry.

Introduction

Noble transition-metal oxides are important catalysts in synthetic chemistry and electrochemistry. At the molecular level, the electronic structures and bonding of simple mononuclear noble transition-metal oxides and dixoygen complexes have been studied both experimentally and theoretically.[1−31] Compared with the intensive studies on the neutral species, experimental reports on the corresponding anions are relatively rare due to the difficulties in preparation and characterization of such highly unstable anionic species.[32] However, some noble transition-metal oxide anions have been studied by the photoelectron spectroscopic method in the gas phase.[33−36] The monoxide and dioxide anions of nickel, palladium, and platinum were investigated by Ramond et al. in the gas phase, in which the electron affinities, spin−orbital splittings, and bond characters of these anions were determined.[33] Recently, Wang and co-workers provided a combined photoelectron spectroscopic and ab initio study on the simple AuO^- and AuO_2^- anions. The AuO_2^- anion was characterized to have a dioxide structure. The $Au(O_2)^-$ anion complex was found to be unbound due to the nonbonding nature between Au^- and O_2.[34]

Laser ablation in conjunction with matrix isolation has proven to be an effective method in producing and trapping unstable charged species for spectroscopic study.[37,38] A large number of transition-metal oxide anions have been prepared in solid noble gas matrixes and were spectroscopically characterized.[38] Recently we have prepared and characterized the FeO_2^- anion in solid argon, which was determined to be a linear species.[39] Theoretical calculations suggested that it was not appropriate to treat this system using single-reference methods such as various DFT and post-HF methods due to the severe symmetry-breaking problems of the reference wave function. However, the experimental results can be effectively reproduced by using the state-averaged multireference MRCI method, which incorporates both dynamical and nondynamical correlations. In this paper, we provide a joint matrix isolation infrared spectroscopic and theoretical study on some noble transition-metal dioxide anions (Rh, Ir, Pt, Au).

Experimental and Computational Details

The experimental setup for pulsed laser ablation and matrix isolation infrared spectroscopic investigation has been described in detail previously.[40] Briefly, the 1064 nm fundamental of a Nd:YAG laser (Continuum, Minilite II, 10 Hz repetition rate, and 6 ns pulse width) was focused onto a rotating noble metal target (Rh, Ir, Pt, and Au) through a hole in a CsI window cooled normally to 6 K by means of a closed-cycle helium refrigerator (ARS, 202N). The ablated metal atoms and electrons were codeposited with O_2 in excess argon onto the CsI window. In general, matrix samples were deposited for 1 h at a rate of approximately 4 mmol/h. The O_2/Ar mixtures were prepared in a stainless steel vacuum line using the standard manometric technique. O_2 (Shanghai BOC, 99.95%) and isotopic $^{18}O_2$ (ISOTEC, 99%) were used without further purification. The infrared absorption spectra of the resulting samples were recorded on a Bruker IFS 66V spectrometer at 0.5 cm^{-1} resolution between 4000 and 450 cm^{-1} using a liquid nitrogen cooled HgCdTe (MCT) detector. Selected samples were subjected to 355 nm laser irradiation or broad-band irradiation using a high-pressure mercury arc lamp with glass filters.

Quantum chemical calculations were performed using the Gaussian 03 program.[41] The three-parameter hybrid functional according to Becke with additional correlation corrections due to Lee, Yang, and Parr (B3LYP)[42,43] was utilized. The 6-311+G(3d) basis set including three d polarization functions was used for the O atom, and the SDD pseudopotential and basis set were used for the Rh, Ir, Pt, and Au atoms.[44,45] The geometries were fully optimized; the harmonic vibrational frequencies were calculated, and zero-point vibrational energies (ZPVEs) were derived.

Results and Discussion

The anions were prepared from codeposition of laser-ablated noble transition-metal atoms and electrons with O_2/Ar mixtures at 6 K. The ablation laser energy is in the range of 15−25 mJ/

* To whom correspondence should be addressed. E-mail: mfzhou@fudan.edu.cn.

10.1021/jp900974w CCC: $40.75
Published on Web 03/31/2009

TABLE 1: Infrared Absorptions (cm^{-1}) of the Observed Transition-Metal Dioxide Anions in Solid Argon

$^{16}O_2$	$^{18}O_2$	$^{16}O_2 + {}^{18}O_2$	$^{16}O_2 + {}^{16}O^{18}O + {}^{18}O_2$	assignment
893.6	855.3	893.6,855.3	−[a], 877.6,855.3	RhO_2^- asym str
891.4	853.1	891.4,853.1		RhO_2^- asym str site
915.7	871.2	915.7,871.2	915.7, 875.0, 871.2	IrO_2^- asym str
925.7	880.7	925.7,880.7		IrO_2 asym str site
847.3	806.2	847.3,806.2	847.3, 843.7, 806.2	PtO_2^- asym str site
836.2	795.5	836.2,795.5	836.2, 832.2, 795.5	PtO_2^- asym str
738.2	702.7	738.2,702.7	738.2, 725.4, 702.7	AuO_2^- asym str

[a] Absorptions unresolved due to band overlap.

pulse depending on the metals used. The metal-independent absorptions due to O_3 (1039.8 cm^{-1}), O_4^- (953.8 cm^{-1}), and O_4^+ (1118.7 cm^{-1}) were observed in all the experiments.[46] Different temperature annealing and wavelength range photolysis studies were done to characterize the absorption species. To help the product identifications, experiments were also performed using the isotope-labeled $^{18}O_2$ and $^{16}O_2 + {}^{18}O_2$ and $^{16}O_2 + {}^{16}O^{18}O + {}^{18}O_2$ mixed samples. The band positions of the anions with different isotopic samples are listed in Table 1.

Au + O_2. The representative infrared spectra from codeposition of laser-ablated gold atoms and electrons with 0.1% O_2 in argon are shown in Figure 1. After 1 h of sample deposition at 6 K, the $Au(O_2)$ complex absorption at 1094.5 cm^{-1} (not shown) and the inserted AuO_2 absorption at 817.7 cm^{-1} were observed.[24] In addition, a new product absorption at 738.2 cm^{-1} (Figure 1a) was also presented. This absorption decreased remarkably when the sample was subjected to UV irradiation with the 355 nm laser light, during which the AuO_2 absorption slightly increased (Figure 1b). The 738.2 cm^{-1} absorption cannot be recovered on subsequent sample annealing to 25 K (Figure 1c), during which the AuO_2 absorption markedly increased. Absorption at 740.5 cm^{-1} which was previously assigned to Au_xO together with the AuO absorption also appeared on sample annealing.[24] In the experiment when the laser-ablated gold atoms and electrons were codeposited with 0.2% $^{18}O_2$ in argon, all the product absorptions were red-shifted. Similar experiments with the $^{16}O_2 + {}^{18}O_2$ and $^{16}O_2 + {}^{16}O^{18}O + {}^{18}O_2$ mixed samples gave diagnostic multiplets as shown in Figure 2, which will be discussed below.

Pt + O_2. In the experiments with a metal platinum target, four metal-dependent absorptions were observed after sample

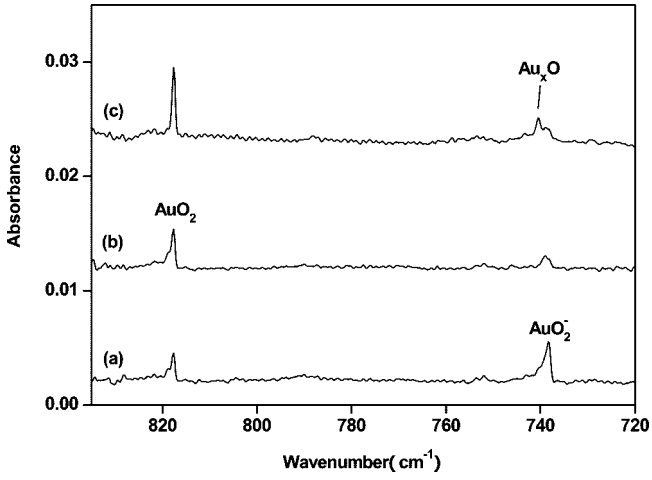

Figure 1. Infrared spectra in the 835−720 cm^{-1} region from codeposition of laser-ablated gold atoms with 0.1% O_2 in argon: (a) 1 h of sample deposition at 6 K, (b) after 10 min of 355 nm irradiation, and (c) after 25 K annealing.

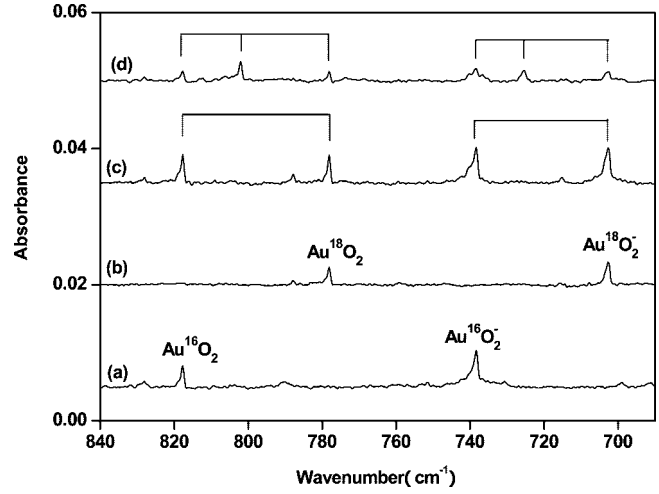

Figure 2. Infrared spectra in the 840−690 cm^{-1} region from codeposition of laser-ablated gold atoms with isotope-labeled dioxygen samples: (a) 0.2% $^{16}O_2$, (b) 0.2% $^{18}O_2$, (c) 0.15% $^{16}O_2$ + 0.15% $^{18}O_2$, and (d) 0.15% $^{16}O_2$ + 0.3% $^{16}O^{18}O$ + 0.15% $^{18}O_2$. Spectra were taken after 1 or 1.5 h of sample deposition.

deposition. Strong absorption at 953.4 cm^{-1} was previously assigned to the antisymmetric stretching mode of the inserted PtO_2 molecule. In addition, weak absorptions at 928.1, 836.2, and 828.0 cm^{-1} were also observed. The 928.1 cm^{-1} absorption together with the 551.1 and 512.5 cm^{-1} absorptions is due to the side-on-bonded $Pt(O_2)$ complex.[19b] The 828.0 cm^{-1} absorption was previously assigned to the PtO molecule.[19] The $Pt(O_2)$ absorptions markedly increased on annealing but were destroyed upon UV irradiation, during which the inserted PtO_2 absorption markedly increased. The newly observed 836.2 cm^{-1} absorption is photosensitive; it decreased upon $300 < \lambda < 580$ nm irradiation and completely disappeared under UV ($250 < \lambda < 300$ nm) irradiation. In contrast to the $Pt(O_2)$ absorptions, which are able to be partially recovered on subsequent annealing, the 836.2 cm^{-1} absorption was not able to be recovered upon subsequent sample annealing after UV irradiation. The infrared spectra in a selected region using different isotopic samples are shown in Figure 3.

Ir + O_2. The infrared spectrum from codeposition of laser-ablated iridium atoms with dioxygen in excess argon at 6 K revealed a strong absorption at 929.0 cm^{-1}, which was previously assigned to the antisymmetric stretching mode of the inserted IrO_2 molecule.[13] Besides the IrO_2 absorption, a photosensitive absorption at 915.7 cm^{-1} was also observed on sample deposition. The 915.7 cm^{-1} absorption was destroyed while the IrO_2 absorption increased markedly when the as-deposited sample was subjected to broad-band irradiation with a mercury arc lamp ($250 < \lambda < 580$ nm). A detailed wavelength-selected experiment suggested that the UV photons in the range of $250 < \lambda < 300$ nm are responsible for the photolysis process. The experiments were repeated using different isotopic samples, with the spectra in a selected region shown in Figure 4.

Rh + O_2. In the experiments with a metal rhodium target, the infrared spectrum after sample deposition was dominated by the strong absorption of rhodium dioxide (900.1 cm^{-1}). Weak absorption at 799.0 cm^{-1} which was previously attributed to the rhodium monoxide molecule was also observed.[6,7] A broad absorption centered at 893.6 cm^{-1} was produced as well upon sample deposition (Figure 5). When the as-deposited sample was subjected to broad-band irradiation ($250 < \lambda < 300$ nm), the 893.6 cm^{-1} absorption disappeared, while the RhO_2 absorption increased remarkably. Sample annealing allows the forma-

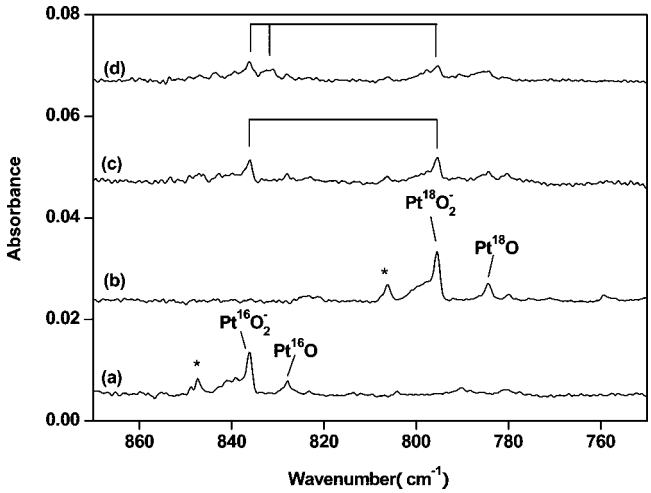

Figure 3. Infrared spectra in the 870−750 cm^{-1} region from codeposition of laser-ablated platinum atoms with isotope-labeled dioxygen samples: (a) 0.5% $^{16}O_2$, (b) 0.5% $^{18}O_2$, (c) 0.25% $^{16}O_2$ + 0.25% $^{18}O_2$, and (d) 0.125% $^{16}O_2$ + 0.25% $^{16}O^{18}O$ + 0.125% $^{18}O_2$. Spectra were taken after 1 h of sample deposition. The asterisks denote the site absorption of PtO_2^-.

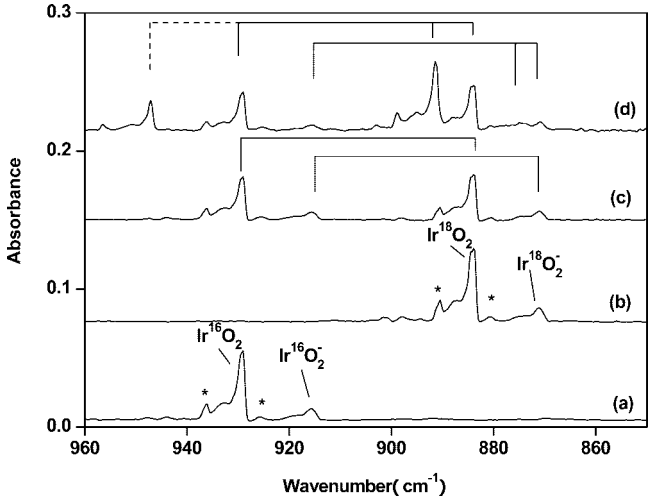

Figure 4. Infrared spectra in the 960−850 cm^{-1} region from codeposition of laser-ablated iridium atoms with isotope-labeled dioxygen samples: (a) 0.5% $^{16}O_2$, (b) 0.5% $^{18}O_2$, (c) 0.25% $^{16}O_2$ + 0.25% $^{18}O_2$, and (d) 0.125% $^{16}O_2$ + 0.25% $^{16}O^{18}O$ + 0.125% $^{18}O_2$. Spectra were taken after 1 h of sample deposition. The asterisks denote the site absorptions of IrO_2 and IrO_2^-.

tion of the $Rh(O_2)$ (959.5 cm^{-1}) as well as the oxygen-rich $(O_2)RhO_2$ complexes.[6,7] Note that both the rhodium dioxide absorption and the 893.6 cm^{-1} absorption were barely observed in previous experiments with relatively low ablation laser energy.[6]

AuO_2^-. The 738.2 cm^{-1} absorption that appeared on sample deposition is photosensitive. It lost most of its intensity when the sample was exposed to the 355 nm laser light irradiation. The photosensitive behavior suggests that the absorber is due to an anionic species. The 738.2 cm^{-1} absorption shifted to 702.7 cm^{-1} when the $^{18}O_2$ sample was used. The resulting $^{16}O/^{18}O$ isotopic frequency ratio of 1.0505 is characteristic of an antisymmetric OAuO stretching vibration. In the spectrum with a mixed $^{16}O_2$ + $^{18}O_2$ sample (Figure 2c), only the pure isotopic counterparts were presented, while a triplet with an intermediate absorption at 725.4 cm^{-1} was observed in the spectrum using a $^{16}O_2$ + $^{16}O^{18}O$ + $^{18}O_2$ mixed sample (Figure 2d). The mixed isotopic spectral features indicate that two equivalent oxygen

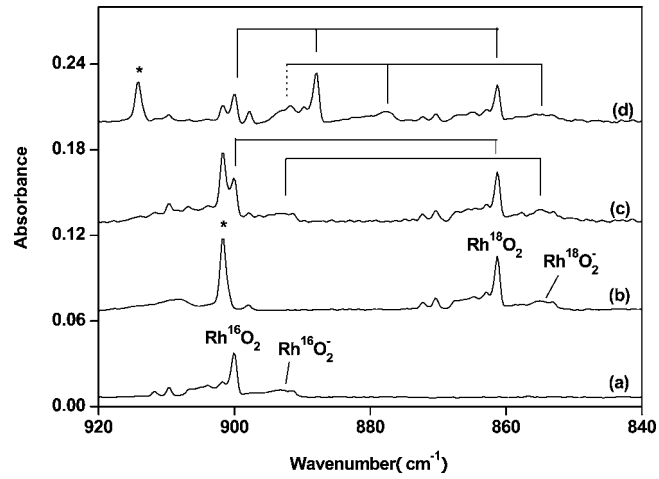

Figure 5. Infrared spectra in the 920−840 cm^{-1} region from codeposition of laser-ablated rhodium atoms with isotope-labeled dioxygen samples: (a) 0.5% $^{16}O_2$, (b) 0.5% $^{18}O_2$, (c) 0.25% $^{16}O_2$ + 0.25% $^{18}O_2$, and (d) 0.125% $^{16}O_2$ + 0.25% $^{16}O^{18}O$ + 0.125% $^{18}O_2$. Spectra were taken after 1 h of sample deposition. The asterisks denote the O_4^- absorptions.

atoms are involved in this vibrational mode, and accordingly, we assign the 738.2 cm^{-1} absorption to the antisymmetric OAuO stretching mode of the AuO_2^- anion. No absorption was observed that can be assigned to the symmetric OAuO stretching vibration of the anion, suggesting that the anion should have a linear or near linear structure. The $^{16}O/^{18}O$ isotopic frequency ratio of the antisymmetric stretching vibration (1.0505) also implies that the AuO_2^- anion should be linear.

The anion assignment is strongly supported by density functional calculations. Consistent with previous theoretical calculations, the gold dioxide anion was predicted to have a triplet ground state with a linear structure (Table 2).[24,34,35] The antisymmetric and symmetric OAuO stretching vibrational modes of the anion were calculated at 750.9 and 706.1 cm^{-1}. The calculated antisymmetric stretching frequency fits the observed value of 738.2 cm^{-1} very well. The symmetric stretching mode is IR inactive. This mode was determined to be 640 ± 40 cm^{-1} from the hot band transitions observed in the photoelectron spectroscopic study on AuO_2^-.[34] The Au−O bond length of the anion was predicted to be 0.073 Å longer than that of the neutral calculated at the same level. The antisymmetric stretching vibrational frequency of the anion was computed to be 133.5 cm^{-1} red-shifted from that of the neutral. Experimentally, the antisymmetric stretching mode of the anion lies 79.5 cm^{-1} lower than that of the AuO_2 neutral observed in solid argon.

PtO_2^-. The photosensitive absorption at 836.2 cm^{-1} in the platinum system is assigned to the antisymmetric OPtO stretching mode of the PtO_2^- anion, which is 117.2 cm^{-1} red-shifted from that of the PtO_2 neutral in solid argon. The $Pt^{18}O_2^-$ anion absorption was observed at 795.5 cm^{-1}. The isotopic spectral features observed in the mixed spectra clearly demonstrated that the absorber involves two equivalent oxygen atoms. The $^{16}O/^{18}O$ isotopic frequency ratio of the antisymmetric stretching vibration (1.0512) suggests that the PtO_2^- anion should be linear or near linear. The intermediate absorption observed at 832.2 cm^{-1} in the spectrum using a $^{16}O_2$ + $^{16}O^{18}O$ + $^{18}O_2$ sample is due to the antisymmetric stretching mode of the $^{16}OPt^{18}O^-$ isotopomer. This absorption is only 4.0 cm^{-1} lower than that of $Pt^{16}O_2^-$, indicating that the infrared inactive symmetric OPtO stretching vibration lies slightly lower than the antisymmetric stretching vibrational mode.

TABLE 2: DFT/B3LYP-Calculated Total Energies (hartrees), Vibrational Frequencies (cm^{-1}), Intensities (km/mol), and Geometries (Bond Length, Å; Bond Angle, deg) of the Anions and Neutrals

		frequency (intensity)			geometry	
molecule	energy	ν_3	ν_2	ν_1	$\angle_{OMO}$	R_{M-O}
RhO_2^- ($^1A_1$, C_{2v})	−261.066377	912.5 (331)	102.0 (1)	846.3 (13)	162.9	1.735
RhO_2 ($^2A_1$, C_{2v})	−260.959868	939.7 (251)	142.9 (13)	918.5 (8)	157.1	1.699
IrO_2^- ($^1\Sigma_g^+$, $D_{\infty h}$)	−254.930415	925.4 (381)	127.0 (0.4 × 2)	956.6 (0)	180.0	1.738
IrO_2 ($^2\Sigma_g^+$, $D_{\infty h}$)	−254.799812	964.0 (278)	58.7 (10 × 2)	1001.5 (0)	180.0	1.717
PtO_2^- ($^2\Pi_g$, $D_{\infty h}$)	−269.879640	861.0 (270)	87.8 (7 × 2)	855.7 (0)	180.0	1.790
PtO_2($^1\Sigma_g^+$, $D_{\infty h}$)	−269.762712	1000.5 (131)	135.6 (2 × 2)	960.1 (0)	180.0	1.719
AuO_2^- ($^3\Sigma_g^-$, $D_{\infty h}$)	−286.233382	750.9 (85)	194.1 (13 × 2)	706.1 (0)	180.0	1.866
AuO_2 ($^2\Pi_g$, $D_{\infty h}$)	−286.076185	884.7 (30)	129.5 (7 × 2)	802.5 (0)	180.0	1.793

Density functional calculations predicted that the platinum dioxide anion has a doublet ground state with a linear structure. The Pt−O bond was calculated to be 1.790 Å, ca. 0.071 Å longer than that of the neutral platinum dioxide molecule calculated at the same level of theory (Table 2). The antisymmetric OPtO stretching vibrational mode of the anion was predicted to be 861.0 cm^{-1} with an isotopic $^{16}O/^{18}O$ frequency ratio of 1.0517, in good agreement with the experimental values. The symmetric stretching mode of the anion was predicted at 855.7 cm^{-1}, only 5.3 cm^{-1} lower than the antisymmetric stretching mode. Although this infrared inactive mode cannot be observed in our experiment, its band position was determined to be 760 ± 35 cm^{-1} via the observed hot bands in a previous photoelectron spectroscopic study.[33]

RhO_2^-. The weak absorption at 893.6 cm^{-1} in the rhodium system is assigned to the antisymmetric ORhO stretching vibration of the RhO_2^- anion isolated in solid argon. Evidence for the assignment of the anion can also be found from a previous matrix isolation experiment on the reaction of thermally evaporated rhodium atoms and O_2, in which no absorption around 893 cm^{-1} was reported.[9] The formation of charged species such as an anion was not expected with thermal evaporation due to the lack of electrons and ions upon the metal evaporation process. The 893.6 cm^{-1} band shifted to 855.3 cm^{-1} with ^{18}O substitution. The $^{16}O/^{18}O$ isotopic frequency ratio of 1.0448 is characteristic of an antisymmetric ORhO stretching vibration. The mixed isotopic spectral features shown in Figure 5 confirmed the assignment of the 893.6 cm^{-1} absorption to the RhO_2^- anion. The $^{16}O/^{18}O$ isotopic frequency ratio of the antisymmetric stretching vibration of the anion (1.0448) is about the same as that of the RhO_2 neutral (1.0451), suggesting that the anion has about the same bond angle as the neutral molecule.

The rhodium dioxide anion was predicted to have a closed shell singlet ground state (Table 2). The linear structure was found to be comparable in energy to the slightly bent C_{2v} isomer (less than 1 kcal/mol). Frequency calculations suggested that the linear isomer is a transition state toward the bending mode. A similar case has been found on the calculation of the neutral rhodium dioxide molecule in the doublet ground state.[6,7] The RhO_2 neutral molecule was determined to be linear on the basis of a matrix ESR measurement.[8] The RhO_2 neutral is isovalent with the FeO_2^- anion, which was characterized to be a linear species.[39] As has been discussed in the FeO_2^- study, calculations with single-reference methods may be unreliable for the treatment of these molecules. The antisymmetric vibrational frequency for the bent RhO_2^- anion was calculated at 912.5 cm^{-1} with an isotopic $^{16}O/^{18}O$ frequency ratio of 1.0456 (Table 3), which are in reasonable agreement with the experimental values. The Rh−O bond length for the rhodium dioxide anion was predicted to be 1.735 Å, 0.036 Å longer than that of the RhO_2 neutral calculated at the same level.

TABLE 3: Comparison between the Observed and Calculated Antisymmetric Vibrational Frequencies (cm^{-1}) and Isotopic Frequency Ratios of the MO_2^- Anions (M = Rh, Ir, Pt, Au)

	frequency		$^{16}O/^{18}O$	
molecule	calcd	obsd	calcd	obsd
RhO_2^- ($^1A_1$, C_{2v})	912.5	893.6	1.0456	1.0448
IrO_2^- ($^1\Sigma_g^+$, $D_{\infty h}$)	925.4	915.7	1.0515	1.0511
PtO_2^- ($^2\Pi_g$, $D_{\infty h}$)	861.0	836.2	1.0517	1.0512
AuO_2^- ($^3\Sigma_g^-$, $D_{\infty h}$)	750.9	738.2	1.0515	1.0505

IrO_2^-. The photosensitive absorption at 915.7 cm^{-1} in the iridium system is assigned to the antisymmetric OIrO stretching vibration of the IrO_2^- anion, which is about 13.3 cm^{-1} red-shifted from the corresponding neutral absorption. The iridium dioxide anion was predicted to have a singlet ground state with a linear structure (Table 2). The antisymmetric vibrational frequency for the linear IrO_2^- anion was calculated at 925.4 cm^{-1} with an isotopic $^{16}O/^{18}O$ frequency ratio of 1.0515. Note that the vibrational frequency of RhO_2^- anion is lower than that of the IrO_2^- anion, identical with the trend observed for the neutrals.[7,13,38b] The similarity between rhodium and iridium is the result of lanthanide contraction, which is common for the second- and third-row transition metals.

Among the metal dioxide systems reported here, it can be found that the antisymmetric stretching vibrational frequencies of the anions are lower than those of the corresponding neutrals. However, the frequency differences for gold (79.5 cm^{-1}) and platinum (106.1 cm^{-1}) are much larger than those of rhodium (6.5 cm^{-1}) and iridium (13.3 cm^{-1}). As has been discussed,[34] the AuO_2 neutral has a linear doublet ($^2\Pi_g$) ground state. The LUMO and SOMO of AuO_2 are doubly degenerate π_g orbitals which are Au−O antibonding in character. Adding an electron to this antibonding π_g orbital elongates the Au−O bond length, which results in a reduction of the stretching vibrational frequency of the anion. The situation for platinum is about the same as that of gold. The PtO_2 neutral has a linear singlet ground state. The LUMO of neutral PtO_2 is an antibonding π orbital, which mainly consists of the O 2p orbital and Pt 5d orbital. Addition of an electron to this orbital of the PtO_2 neutral results in the $^2\Pi_g$ ground-state PtO_2^- anion. In contrast to AuO_2 and PtO_2, in which the electron is added into an antibonding orbital of the neutral to give the anion, the electron is filled into an orbital of the neutral which is largely nonbonding in the case of rhodium and iridium. The neutral RhO_2 molecule has a doublet ground state. Bonding analysis indicated that the SOMO of the RhO_2 neutral is a nonbonding orbital mainly derived from the 5s atomic orbital of rhodium. Apparently, addition of an electron to this nonbonding orbital will not change the bond strength of RhO_2 significantly. As a result, the antisymmetric stretching vibrational frequency of the anion is only slightly lower than that of the neutral.

The metal dioxide anions could be formed either via electron capture by the neutral metal dioxide molecules during the codeposition process or via reactions between metal atoms and dioxygen anions. Although the O_2^- anion cannot be detected by infrared absorption spectroscopy, its formation is confirmed by the observation of O_4^- anion on sample deposition. The O_4^- anion absorption is favored with relatively low ablation laser energy. Our experimental investigations demonstrated that the metal dioxide anions could only be observed with relatively high ablation laser energy, during which the corresponding metal dioxide neutrals were observed upon sample deposition. This observation suggests that the metal dioxide anions were mainly formed via electron capture by the metal dioxide neutrals during the cocondensation process. All four of the electron attachment processes were predicted to be exothermic by the DFT/B3LYP calculations:

$$RhO_2\ (^2A_1) + e \rightarrow RhO_2^-\ (^1A_1) \qquad \Delta E = -2.90\ \text{eV}\ (-66.8\ \text{kcal/mol}) \quad (1)$$

$$IrO_2\ (^2\Sigma_g^+) + e \rightarrow IrO_2^-\ (^1\Sigma_g^+) \qquad \Delta E = -3.55\ \text{eV}\ (-82.0\ \text{kcal/mol}) \quad (2)$$

$$PtO_2\ (^1\Sigma_g^+) + e \rightarrow PtO_2^-\ (^2\Pi_g) \qquad \Delta E = -3.18\ \text{eV}\ (-73.4\ \text{kcal/mol}) \quad (3)$$

$$AuO_2\ (^2\Pi_g) + e \rightarrow AuO_2^-\ (^3\Sigma_g^-) \qquad \Delta E = -4.28\ \text{eV}\ (-98.6\ \text{kcal/mol}) \quad (4)$$

The platinum and gold dioxide anions have been investigated in the gas phase using photoelectron spectroscopy. The adiabatic electron affinity for platinum dioxide was measured to be 2.677 ± 0.005 eV, which is about 0.5 eV lower than our theoretically predicted value.[33] The electron affinity for the gold dioxide molecule was also determined recently. The experimental value around 3.40 eV is about 0.8 eV lower than the 4.28 eV value calculated here.[34] It has been suggested that DFT methods can be used to estimate the electron affinities for molecular anions but usually gave values slightly higher than the experimentally determined affinities.[47,48]

Conclusions

Laser-ablated rhodium, iridium, platinum, and gold atoms reacted with O_2 in excess argon during condensation to form the metal dioxide molecules as the major products. In addition, the metal dioxide anions were also formed via capture of ablated electrons by the neutral molecules. Photosensitive absorptions at 893.6, 915.7, 836.2, and 738.2 cm^{-1} were assigned to the antisymmetric stretching vibrations of the RhO_2^-, IrO_2^-, PtO_2^-, and AuO_2^- anions, respectively, on the basis of isotopic splittings and density functional theory frequency calculations. The calculations predicted that the third-row transition-metal dioxide anions IrO_2^-, PtO_2^-, and AuO_2^- have singlet, doublet, and triplet ground states with linear structures, while the RhO_2^- anion was predicted to have a slightly bent geometry. The observed antisymmetric stretching vibrational frequencies of the anions are lower than those of the corresponding neutrals. The frequency differences for gold and platinum are much larger than those of rhodium and iridium. Bonding analysis showed that the electron is added into an antibonding orbital of the neutral to give the anion for AuO_2 and PtO_2, whereas the electron is filled into an orbital of the neutral which is largely nonbonding in the case of rhodium and iridium.

Acknowledgment. Financial support from the National Basic Research Program of China (Grant No. 2007CB815203) and the National Natural Science Foundation of China (Grant No. 20773030) is gratefully acknowledged.

References and Notes

(1) Huber, K. P.; Herzberg, G. *Molecular Spectra and Molecular Structure IV: Constants of Diatomic Molecules*; Van Nostrand Reinhold: New York, 1979.
(2) Gengler, J.; Ma, T.; Adam, A. G.; Steimle, T. C. *J. Chem. Phys.* **2007**, *126*, 134304.
(3) (a) Heuff, R. F.; Fougere, S. G.; Balfour, W. J. *J. Mol. Spectrosc.* **2005**, *231*, 99. (b) Jensen, R. H.; Fougere, S. G.; Balfour, W. J. *Chem. Phys. Lett.* **2003**, *370*, 106. (c) Heuff, R. F.; Balfour, W. J.; Adam, A. G. *J. Mol. Spectrosc.* **2002**, *216*, 136.
(4) Li, X.; Wang, L. S. *J. Chem. Phys.* **1998**, *109*, 5264.
(5) Raziunas, V.; Macur, G.; Katz, S. *J. Chem. Phys.* **1965**, *43*, 1010.
(6) Yang, R.; Gong, Y.; Zhou, H.; Zhou, M. F. *J. Phys. Chem. A* **2007**, *111*, 64.
(7) Citra, A.; Andrews, L. *J. Phys. Chem. A* **1999**, *103*, 4845.
(8) Van Zee, R. J.; Hamrick, Y. M.; Li, S.; Weltner, W., Jr. *J. Phys. Chem.* **1992**, *96*, 7247.
(9) (a) Hanlan, A. J. L.; Ozin, G. A. *Inorg. Chem.* **1977**, *16*, 2848. (b) Hanlan, A. J. L.; Ozin, G. A. *Inorg. Chem.* **1977**, *16*, 2857. (c) Huber, H.; Klotzbuecher, W.; Ozin, G. A.; Vander Voet, A. *Can. J. Chem.* **1973**, *51*, 2722.
(10) Song, P.; Guan, W.; Yao, C.; Su, Z. M.; Wu, Z. J.; Feng, J. D.; Yan, L. K. *Theor. Chem. Acc.* **2007**, *117*, 407.
(11) (a) Siegbahn, P. E. M. *Chem. Phys. Lett.* **1993**, *201*, 15. (b) Siegbahn, P. E. M. *J. Phys. Chem.* **1993**, *97*, 9096.
(12) Mains, G. J.; White, J. M. *J. Phys. Chem.* **1991**, *95*, 112.
(13) Citra, A.; Andrews, L. *J. Phys. Chem. A* **1999**, *103*, 4182.
(14) (a) Jansson, K.; Scullman, R. *J. Mol. Spectrosc.* **1972**, *43*, 208. (b) Jansson, K.; Scullman, R. *Ber. Bunsen-Ges.* **1978**, *82*, 92.
(15) Yao, C.; Guan, W.; Song, P.; Su, Z. M.; Feng, J. D.; Yan, L. K.; Wu, Z. J. *Theor. Chem. Acc.* **2007**, *117*, 115.
(16) Citir, M.; Metz, R. B.; Belau, L.; Ahmed, M. *J. Phys. Chem. A* **2008**, *112*, 9584.
(17) Frum, C. I.; Engleman, R., Jr.; Bernath, P. F. *J. Mol. Spectrosc.* **1991**, *150*, 566.
(18) (a) Sassenberg, U.; Scullman, R. *Phys. Scr.* **1983**, *28*, 139. (b) Sassenberg, U.; Scullman, R. *J. Mol. Spectrosc.* **1977**, *68*, 331. (c) Jansson, K.; Scullman, R. *J. Mol. Spectrosc.* **1976**, *61*, 299. (d) Scullman, R.; Sassenberg, U.; Nilsson, C. *Can. J. Phys.* **1975**, *53*, 1991.
(19) (a) Bare, W. D.; Citra, A.; Chertihin, G. V.; Andrews, L. *J. Phys. Chem. A* **1999**, *103*, 5456. (b) Danset, D.; Manceron, L.; Andrews, L. *J. Phys. Chem. A* **2001**, *105*, 7205.
(20) Steimle, T. C.; Jung, K. Y.; Li, B.-Z. *J. Chem. Phys.* **1995**, *103*, 1767.
(21) Chung, S.-C.; Krueger, S.; Pacchioni, G.; Roesch, N. *J. Chem. Phys.* **1995**, *102*, 3695.
(22) (a) O'Brien, L. C.; Oberlink, A. E.; Roos, B. O. *J. Phys. Chem. A* **2006**, *110*, 11954. (b) O'Brien, L. C.; Hardimon, S. C.; O'Brien, J. J. *J. Phys. Chem. A* **2004**, *108*, 11302.
(23) Okabayashi, T.; Koto, F.; Tsukamoto, K.; Yamazaki, E.; Tanimoto, M. *Chem. Phys. Lett.* **2005**, *403*, 223.
(24) (a) Wang, X. F.; Andrews, L. *J. Phys. Chem. A* **2001**, *105*, 5812. (b) Citra, A.; Andrews, L. *J. Mol. Struct.: THEOCHEM* **1999**, *489*, 95.
(25) Kasai, P. H.; Jones, P. M. *J. Phys. Chem.* **1986**, *90*, 4239.
(26) Howard, J. A.; Sutcliffe, R.; Mile, B. *J. Phys. Chem.* **1984**, *88*, 4351.
(27) Griffiths, M. J.; Barrow, R. F. *J. Chem. Soc., Faraday Trans. 2* **1977**, *73*, 943.
(28) McIntosh, D.; Ozin, G. A. *Inorg. Chem.* **1976**, *15*, 2869.
(29) Tielens, F.; Gracia, L.; Polo, V.; Andres, J. *J. Phys. Chem. A* **2007**, *111*, 13255.
(30) Okumura, M.; Kitagawa, Y.; Haruta, M.; Yamaguchi, K. *Chem. Phys. Lett.* **2001**, *346*, 163.
(31) Schwerdtfeger, P.; Dolg, M.; Schwarz, W. H. E.; Bowmaker, G. A.; Boyd, P. D. W. *J. Chem. Phys.* **1989**, *91*, 1762.
(32) Simons, J. *J. Phys. Chem. A* **2008**, *112*, 6401.
(33) Ramond, T. M.; Davico, G. E.; Hellberg, F.; Svedberg, F.; Salén, P.; Söderqvist, P.; Lineberger, W. C. *J. Mol. Spectrosc.* **2002**, *216*, 1.
(34) Zhai, H. J.; Bürgel, C.; Bonacic-Koutecky, V.; Wang, L. S. *J. Am. Chem. Soc.* **2008**, *130*, 9156.

(35) (a) Stolcic, D.; Fischer, M.; Ganteför, G.; Kim, Y. D.; Sun, Q.; Jena, P. *J. Am. Chem. Soc.* **2003**, *125*, 2848. (b) Sun, Q.; Jena, P.; Kim, Y. D.; Fischer, M.; Ganteför, G. *J. Chem. Phys.* **2004**, *120*, 6510.

(36) Ichino, T.; Gianola, A. J.; Andrews, D. H.; Lineberger, W. C. *J. Phys. Chem. A* **2004**, *108*, 11307.

(37) (a) Zhou, M. F.; Andrews, L.; Bauschlicher, C. W., Jr. *Chem. Rev.* **2001**, *101*, 1931. (b) Andrews, L.; Citra, A. *Chem. Rev.* **2002**, *102*, 885.

(38) (a) Zhou, M. F.; Andrews, L. *J. Chem. Phys.* **1999**, *111*, 4230. (b) Zhou, M. F.; Citra, A.; Liang, B. Y.; Andrews, L. *J. Phys. Chem. A* **2000**, *104*, 3457. (c) Zhou, M. F.; Andrews, L.; Ismail, N.; Marsden, C. *J. Phys. Chem. A* **2000**, *104*, 5495. (d) Dong, J.; Wang, Y.; Zhou, M. F. *Chem. Phys. Lett.* **2002**, *364*, 511. (e) Zhou, M. F.; Shao, L. M.; Miao, L. *J. Phys. Chem. A* **2002**, *106*, 6483.

(39) Li, Z. H.; Gong, Y.; Fan, K. N.; Zhou, M. F. *J. Phys. Chem. A* **2008**, *112*, 13641.

(40) Wang, G. J.; Zhou, M. F. *Int. Rev. Phys. Chem.* **2008**, *27*, 1.

(41) Frisch, M. J.; Trucks, G. W.; Schlegel, H. B.; Scuseria, G. E.; Robb, M. A.; Cheeseman, J. R.; Montgomery, J. A., Jr.; Vreven, T.; Kudin, K. N.; Burant, J. C.; Millam, J. M.; Iyengar, S. S.; Tomasi, J.; Barone, V.; Mennucci, B.; Cossi, M.; Scalmani, G.; Rega, N.; Petersson, G. A.; Nakatsuji, H.; Hada, M.; Ehara, M.; Toyota, K.; Fukuda, R.; Hasegawa, J.; Ishida, M.; Nakajima, T.; Honda, Y.; Kitao, O.; Nakai, H.; Klene, M.; Li, X.; Knox, J. E.; Hratchian, H. P.; Cross, J. B.; Adamo, C.; Jaramillo, J.; Gomperts, R.; Stratmann, R. E.; Yazyev, O.; Austin, A. J.; Cammi, R.; Pomelli, C.; Ochterski, J. W.; Ayala, P. Y.; Morokuma, K.; Voth, G. A.; Salvador, P.; Dannenberg, J. J.; Zakrzewski, V. G.; Dapprich, S.; Daniels, A. D.; Strain, M. C.; Farkas, O.; Malick, D. K.; Rabuck, A. D.; Raghavachari, K.; Foresman, J. B.; Ortiz, J. V.; Cui, Q.; Baboul, A. G.; Clifford, S.; Cioslowski, J.; Stefanov, B. B.; Liu, G.; Liashenko, A.; Piskorz, P.; Komaromi, I.; Martin, R. L.; Fox, D. J.; Keith, T.; Al-Laham, M. A.; Peng, C. Y.; Nanayakkara, A.; Challacombe, M.; Gill, P. M. W.; Johnson, B.; Chen, W.; Wong, M. W.; Gonzalez, C.; Pople, J. A. *Gaussian 03*, revision B.05; Gaussian, Inc.: Pittsburgh, PA, 2003.

(42) Becke, A. D. *J. Chem. Phys.* **1993**, *98*, 5648.

(43) Lee, C.; Yang, W.; Parr, R. G. *Phys. Rev. B* **1988**, *37*, 785.

(44) (a) McLean, A. D.; Chandler, G. S. *J. Chem. Phys.* **1980**, *72*, 5639. (b) Krishnan, R.; Binkley, J. S.; Seeger, R.; Pople, J. A. *J. Chem. Phys.* **1980**, *72*, 650.

(45) (a) Dolg, M.; Stoll, H.; Preuss, H. *J. Chem. Phys.* **1989**, *90*, 1730. (b) Andrae, D.; Haussermann, U.; Dolg, M.; Stoll, H.; Preuss, H. *Theor. Chim. Acta* **1990**, *77*, 123.

(46) (a) Zhou, M. F.; Hacaloglu, J.; Andrews, L. *J. Chem. Phys.* **1999**, *110*, 9450. (b) Chertihin, G. V.; Andrews, L. *J. Chem. Phys.* **1998**, *108*, 6404.

(47) Galbraith, J. M.; Schaefer, H. F., III. *J. Chem. Phys.* **1996**, *105*, 862.

(48) Zhang, L. N.; Dong, J.; Zhou, M. F. *J. Chem. Phys.* **2000**, *113*, 8700.

JP900974W